

## Physical Properties of Film Alloys Based on Ferromagnetic and Noble Metals (Review). I. Film Materials Based on Fe and Ag or Au

L.V. Odnodvoretz, I.Yu. Protsenko\*, Yu.M. Shabelnyk, M.O. Shumakova, O.P. Tkach

Sumy State University, 2, Rymaskogo-Korsakova st., 40007 Sumy, Ukraine

(Received 04 May 2016; published online 03 October 2016)

The results of analysis of literature and own data on the phase composition, electrophysical and magnetoresistive properties of granular film alloys based on Fe and Ag or Au are present. Analyzed the question about system designations of film structures, which adopted in the literature and does not meet their physical nature in its original state and after annealing. A new system of signs ordered and disordered solid solutions without and with the presence elements of granular state; quasigranular alloys, in which the role played granules of ferromagnetic island films; intermetallic and others was proposed. It is established that the electrophysical properties (temperature coefficient of resistance – TCR and strain coefficient – SC) defined conductive matrix as s.s., and in nanoscale granules realized the ballistic conductivity mechanism that does not affect the value of TCR and SC. In granular film alloys s.s. Au (Fe) + granules at the plastic deformation observed abnormal increase in comparison with the elastic deformation value SC (10 times) at a concentration  $c_{Fe} \cong 55-75$  at. %.

**Keywords:** Nanodimensional film materials, Electrophysical properties, Magnetoresistive properties, Granular film alloys, Disordered and ordered solid solution.

DOI: [10.21272/jnep.8\(3\).03034](https://doi.org/10.21272/jnep.8(3).03034)

PACS numbers: 75.70. – i, 75.47.Np

### 1. INTRODUCTION

The discovery [1] a new type of material – granulated film alloys contributed to the further theorem and experimental study not only the phenomenon of giant magnetoresistance (GMR), but magnetic and electrophysical properties, such as resistivity ( $\rho$ ), thermal coefficient of resistance (TCR –  $\beta$ ), strain coefficient (SC –  $\gamma$ ), magnetoresistance (MR), the magnetization (M) et. al. Formation of the magnetic granules Co or Fe in nonferromagnetic matrix as a solid solution (s.s.) atoms of paramagnetic metals (for example, Cu, Ag and Au) causes the appearance of new effects of the spin-dependent scattering of electrons (SDSE) compared with multilayers without elements of granular state. It goes that when the magnitude of GMR multilayers affect processes such as spin-orbit scattering, exchange scattering by paramagnetic impurities, electron-magnon scattering (see, for example, [2]).

In the transition to single-layer film granular alloys is not expected great value GMR, though, along with the mechanisms listed above scattering of electrons there are two new – scattering on the surface and in the granular volumes [3], which leads to further reduction (spin-diffusion length path of electrons ( $\lambda_{0^{s-d}}$ ). In the quasi-classical theory [3] assumed that the value  $\lambda_{0^{s-d}}$  smaller structural inhomogeneities (average granular radius ( $r_0$ ) and non-magnetic between the granules gaps or fragments s.s. ( $\Delta l_{ss}$ ) between the two adjacent granules). With this assumption should not expect a large calculated value GMR compared with GMR, which received within the quantum formalism Kubo, which assumed that  $\lambda_{0^{s-d}} \gg r_0$ .

In [4] in the framework of the microscopic approach was theoretically shown that in granular films is likely to be the effect of anisotropy (the order of several percent) us MR and so GMR, that their value depends on

the orientation of the current in the film plane relative magnetization.

The reason for AMR and AGMR is sponsored anisotropy of a resistance ferromagnetic material in the film. The authors [5] described the negative effect of GMR in granular microwires, which is associated with SDSE to localized magnetic moments of the atoms in the inter-granular intervals.

We proposed [6, 7] the phenomenological models for electrophysical properties of granular single-layer films, which, in its simplicity, allow for comparison with experiments and predicting values  $\rho$ , TCR and SC.

Based ratios for TCR can be represented as follows:

$$\beta = \beta_{ss} - \frac{4\beta_g \rho_g}{4\rho_g + \alpha\rho_{ss}} - \frac{\alpha\beta_{ss}\rho_{ss}}{4\rho_g + \alpha\rho_{ss}} + \frac{\beta_g \rho_g + \alpha\beta_{ss}\rho_{ss}}{\rho_g + \alpha\rho_{ss}}, \quad (1)$$

where the indices g and ss indicate the granular material or s.s.

The value

$$\alpha = \frac{\Delta l_{ss}}{r_0}$$

is the coefficient of granulation that calculated based on electron microscopic studies and can be largely mixing of atoms of magnetic and nonmagnetic components.

Note that the same degree of mixing of atoms can be variable

$$\frac{d_{h_1 k_1 l_1}^{NM} + d_{h_2 k_2 l_2}^M}{2},$$

\* [i.protsenko@aph.sumdu.edu.ua](mailto:i.protsenko@aph.sumdu.edu.ua)

where  $d$  – interplane distance;  $hkl$  – Miller indices; NM and  $M$  – non-magnetic and magnetic metal, as proposed in [8].

In the extreme case the value  $\alpha$  ratio (1) can be represented as [9, 10]:

$$\begin{aligned} \beta &\cong \beta_{ss} - \frac{4\beta_g \rho_g}{\alpha \rho_{ss}}, \alpha \gg 1; \beta \cong \beta_{ss} - \frac{\alpha \beta_{ss} \rho_{ss}}{4\rho_g}, \alpha \ll 1; \\ \beta &\cong \beta_{ss} - \frac{4\beta_g \rho_g + \beta_{ss} \rho_{ss}}{4\rho_g + \rho_{ss}} + \frac{\beta_g \rho_g + \beta_{ss} \rho_{ss}}{\rho_g + \rho_{ss}}, \alpha \cong 1. \end{aligned} \quad (2)$$

For SC in three extreme cases may be written such ratios [7]:

$$\begin{aligned} \gamma_l^p &\cong \gamma_{l^{ps}}^p \left( 1 - \frac{\alpha(1-\gamma_{l^{ps}}^p)}{4\alpha + B} \right), \alpha \gg 1; \\ \gamma_l^p &\cong \gamma_{l^{ps}}^p \left( 1 - \frac{\rho_{ss} \rho_g}{\rho_g^2 (4+B)} \right), \alpha \ll 1; \\ \gamma_l^p &\cong \gamma_{l^{ps}}^p \left( 1 - \frac{\rho_{ss} \left[ \rho_g + \rho_{ss} (1-\gamma_{l^{ps}}^p) \right]}{(\rho_g + \rho_{ss})^2 \left( 4 + \frac{B \rho_{ss}}{\rho_g + \rho_{ss}} \right)} \right), \alpha \cong 1, \end{aligned} \quad (3)$$

where the index  $l$  indicates the longitudinal deformation; the superscripts  $\rho_g$  and  $\rho_{ss}$  mean that the value  $\eta$  expressed through  $\rho_g$  or  $\rho_{ss}$ ;  $B = 4,65\pi$ .

Along with theoretical studies, undefined accumulated considerable experimental concerning the physical properties of granular films. We note the few works that are conceptual character. Primarily, classic work [11], which set out the concept of antiferromagnetic interaction between layers in multilayer film materials, including and based on Co and Au, in a film that is a system in which, as will become clear (see, for example, [12]) can be realized elements of granular state.

The research of fundamental character were carried by the authors [13] for effect of material selection and background impurity on interface property. We will also bear in mind the great volume of experimental studies from theme of our work, which presented in reviews [12, 14-17].

Finally, it is necessary to focus of attention on two circumstances which are relevant to granular alloy films. First, we clearly distinguish granular solid solutions, which are formed in systems with limited solubility magnetic components in the fcc lattice of Cu, Ag or Au and grain boundary diffusion limited volume of magnetic atoms causes formation of separate components segregation of atoms that are not dissolved in the lattice non-magnetic components in nanoscale form of granules, usually spherical.

Such granular alloy film (GFA) can be formed by simultaneous condensation of components ( $\text{Me}_1 + \text{Me}_2$ )/S or with the appropriate thermal processing two- or multilayer (for example,  $(\text{Me}_3/\text{Me}_2/\text{Me}_1/\text{S})$ ) film systems. At the same time we use the term "quasi granular films" (QGF), which are formed by condensation island films (IF) magnetic components on a layer of non-magnetic components, followed by the upper layer of non-magnetic components.

Thus, the magnetic islands (we should call them quasigranules), which likely will irregular form, implemented in leading matrix (note that this may be a dielectric (D) matrix). Note that the authors [17] also consider three groups of granular films: magnetic  $\text{Me}_1 - \text{Me}_2$  granular films (1); magnetic  $\text{Me}_1 - \text{insulator}$  granular films (2) and magnetic nanocluster – assembled in granular films (3). In our opinion more correct group (3) call quasigranular film systems. In both cases, the beads and quasigranules will have a certain size distribution. The relatively large or small granules and islands will give a different contribution to the value of GMR, because nanoscale granules and islands may have superparamagnetic properties [12]. This is the conclusion the authors [18] at the study of GMR in granular films based on Co and Ag.

Second, in the references there is a terminological confusion in the indication of structural phase composition of samples in the initial and final state.

In our view, wrong to designate the samples in the initial state symbols alloy  $(\text{Me}_1-\text{Me}_2)$  or intermetallic  $(\text{Me}_1)_x(\text{Me}_2)_y$ , in, as do many authors.

We will adhere to the following designations:

Initial sample	The sample in the end
$(\text{Me}_1 + \text{Me}_2)/\text{S}$ – simultaneous condensation of two metals; $\text{Me}_1/\text{Me}_2/\text{S}$ – double-layer system; $[\text{Me}_1/\text{Me}_2]_n/\text{S}$ – multilayer	s.s. $(\text{Me}_1)$ or s.s. $\text{Me}_1(\text{Me}_2)$ – disordered solid solution based on $\text{Me}_1$ ; s.s. $(\text{Me}_1, \text{Me}_2)$ – ordered s.s. based on $\text{Me}_1$ ; s.s. $(\text{Me}_1) + \text{G}$ or s.s. $\text{Me}_1(\text{Me}_2) + \text{G}$ – granular disordered s.s. based on $\text{Me}_1$ ; s.s. $(\text{Me}_1, \text{Me}_2) + \text{G}$ – granular ordered s.s. based on $\text{Me}_1$
$(\text{Me}_1$ or D)/island film $\text{Me}_2/(\text{Me}_1$ or D)/S – nanocomposite material with separate layer of magnetic islandes	Nanocomposite material with implementation in metal $\text{Me}_1$ or dielectric D of island $\text{Me}_2$
$(\text{Me}_1 + \text{Me}_2)/\text{S}$ , $\text{Me}_1/\text{Me}_2/\text{S}$ – single or double-layer system	$(\text{Me}_1)_x(\text{Me}_2)_y$ – intermetallide; s.s. $\text{Me}_1(\text{Me}_2)$ or s.s. $(\text{Me}_1, \text{Me}_2)$
$[\text{Me}_1/\text{Me}_2]_n/\text{S}$ – multilayer	$(\text{Me}_1)_x(\text{Me}_2)_y$ – intermetallide; s.s. $\text{Me}_1(\text{Me}_2)$ or s.s. $(\text{Me}_1, \text{Me}_2)$ based on component, which enter into a chemical bond

## 2. FILM MATERIALS BASED ON Fe AND Ag

### 2.1 Structural-phase State

Although the that the question about structural-phase state discussed in the earliest studies (see, for example, [14, 19-21]), the most detailed studies, in our opinion, were carried by the authors of [22, 23]. First of all, the authors [22, 23] observation the formation of limited s.s. Fe atoms in the fcc lattice Ag at a concentration  $c_{Fe}$  to 48 [22] or 38 at. % [23]. Lattice parameter s.s. Ag(Fe), according to [23] decreases from 0.4078 to 0.4029 nm at the increasing  $c_{Fe}$  from 0 to 38 at. %. The authors emphasize that similar results were obtained previously by other authors.

Very important is the fact that the authors [23] carried research of phase composition films at  $c_{Fe} = 60-90$  at. %, which together with the data of [22], can almost completely covers the whole range of concentrations atoms Fe.

As installed authors [22] at high concentrations of Fe atoms forming the second s.s.  $\alpha$ -Fe(Ag) from bcc lattice parameter slightly higher than in the bulk  $\alpha$ -Fe. At a concentration of  $c_{Fe} \cong 49$  at. % there are two phases s.s. Ag(Fe) and s.s.  $\alpha$ -Fe(Ag). Note that a similar phase composition observed in films based on Fe and Au (see, section 3.1), and the films s.s. Ag(Fe), unlike s.s.  $\alpha$ -Fe(Ag) have a granular structure. It is important, and also noted that the structure granulated formed regardless of the methods of condensation and initial structural state.

Based on literature data, we can argued that most authors use magnetron sputtering method [14, 19, 23, 24-29] at the layered or simultaneous condensation of individual components. In addition, it must be emphasized that the works only authors [14, 19, 23, 29] were analyzed by XRD phase composition, and the conclusion of granular state was made based on observation GMR effect [14, 19]. The exception in this case could be the work [23], which are the results of microscopic studies from film s.s. and granular film s.s. (grain size from 10 to 40 nm). These results only qualitatively correlated with data [29]: at  $c_{Fe} < 20$  at.% is formed s.s. without granular state elements; at 20 at. %  $< c_{Fe} < 32$  at. % in s.s. there is  $\alpha$ -Fe granules very small, and at  $c_{Fe} > 32$  at. % granules achieve dimensions about 10 nm.

According to the data of articles [22, 30, 31] at the laser evaporation the film materials based on Fe and Ag may be granular structure. Some advantages of this method is that the substrate is present droplet phase, which is characteristic of bulk alloy from which formed film.

At the electron beam evaporation and condensation layer [32, 33] formed multilayer structure and micro-structure of the diffraction pattern which is shown in Fig. 1. The authors [21] formed granular film system by ion sputtering with an average grain size  $\alpha$ -Fe – 11 nm.

The method of ion beam mixing [34, 35] also allows can also form a granular system, and in the case [35] as with granules  $\alpha$ -Fe, and Ag with size 10-20 nm. Analiz of literature data indicates that granular film can be formed by methods of molecular epitaxy [36], sol-gel method [37] or codeposition of Fe cluster and Ag atoms [20] (obviously, in the last case is a quasigranulare system).

Some dissonance is the results of work [38], in which the authors not failed to form a granular s.s. at the preparation of films by method of double-electrode electrodeposition. Mössbauer spectra indicated that the Fe atoms are totally dispersed in the Ag matrix.

### 2.2 Electrophysical Properties

In the literature known a very limited number of results about electrical properties of granular films based on Fe and Ag. It goes on the temperature dependence of the resistance, TCR and concentration

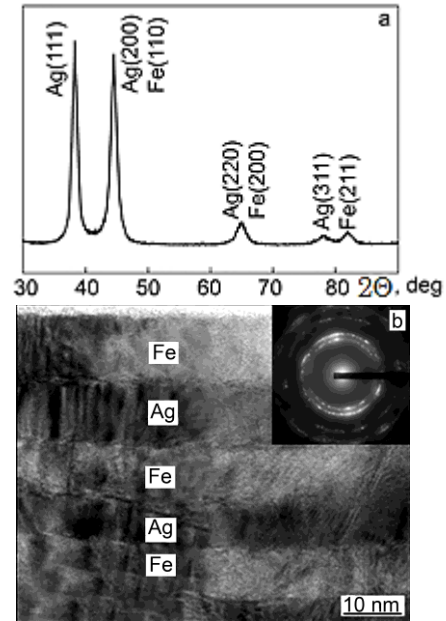


**Fig. 1** – XRD patterns (a) cross-section TEM image for multilayer [Fe/Ag]. From the work [33]

dependence of strain effect. One of these works [39] devoted to the study temperature dependence of conductivity for epitaxial multilayer system Fe/Ag on substrates GaAs (100) and GaAs (110), which is regarded us good candidates of spin-polarized injection of electrons in GaAs-heterostructure. Thus, the work [39] has no direct relationship to the subject of our consideration.

To some extent, the same conclusion can be made about work [31], which presents the results of studies of the temperature dependence of resistance (temperature range 50-300 K) of granular films with concentration  $c_{Fe} = 20-70$  at. %, which received of simultaneous laser evaporation. Feature of research [31] is that the film condensed into two different types of substrate p-type Si, B-doped of atoms with a layer of SiO<sub>2</sub> (thickness 1-2 nm): substrate thickness of 200  $\mu$ m low resistivity ( $1,5 \cdot 10^{-4}$  Ohm-m) and substrate with thickness is 380  $\mu$ m thick with high resistivity ( $7-25 \cdot 10^{-2}$  Ohm-m). The authors emphasize that between substrate and the layer of granular films (120-150 nm thickness) formed amorphous interface with Ag, Fe and Si atoms with thickness 7-10 nm, and that such an interface formed by condensation of granulated alloy based on Co and Ag. The authors observed the different nature of the temperature dependence of the resistance granular films: the low-resistance substrate in the range of 70-212 K monotonically increases, as in the case of high substrate

throughout the temperature range (TCR value of approximately  $3 \cdot 10^{-4} \text{ K}^{-1}$ ), but starting from temperature  $T > 200 \text{ K}$ , sharply reduced (TCR  $\cong -8 \cdot 10^{-3} \text{ K}$ ). After annealing films to 370 and 420 K temperature dependence of character in both cases does not change, only about twice the value decreases resistance. The authors believe that the role of interface is vital in the temperature – dependent current switching phenomena, deviation the current from thin film to the substrate above a certain temperature.

The authors [32] studied the magnetic and transport properties of granular multilayers with different thickness spacer Ag:  $[\text{Ag}(2,6)/\text{Fe}(0,2)]_{75}\text{Ag}(0,8 - 2,6)/\text{Si}(111)$ , where in brackets the thickness of the layers in nanometers. At a concentration of 10 at.% Fe authors observed to be dispersed in fcc Ag matrix or in disordered regions. The resistivity of granular composite authors [32] presented in the form of Matthiessen rule taking into account the electron-magnon scattering:

$$\rho(T, B) = \rho_0 + \rho_{ph}(T) + \rho_m(T, B), \quad (4)$$

where  $\rho_0$  – residual resistance, which approximately equal  $\rho(4,2 \text{ K}; B)$ ;  $\rho_{ph}(T)$  – contribution to the resistivity of the electron-phonon interaction;  $\rho_m(T, B)$  – contribution to the resistivity of the electron-magnon interaction.

The function  $\rho_{ph}(T)$  expressed as the ratio of the Bloch-Gruneisen:

$$\rho_{ph}(T) = a_1 \left( \frac{T}{\Theta_D} \right)^3 \int_0^{\Theta_D/T} \frac{x^2 dx}{e^x - 1}, \quad (5)$$

where  $a_1$  – angular of dependency ratio  $\rho(T, B)$  at the  $B \rightarrow 0$ ;  $\Theta_D$  – Debay temperature.

The calculation  $\rho_m(T, B)$  performed on ratio:

$$\rho_m(T, B) = a_2 \left[ s - \left( s + \frac{1}{2} \right) \coth \frac{(2s+1)g\mu_B B}{2kT} + \frac{1}{2} \coth \frac{g\mu_B B}{2kT} \right], \quad (6)$$

where  $s$  – the total value of spin;  $\mu_B$  – the Bohr magneton;  $B$  – magnetic field.

In some credibility in precision calculations (for example, the authors value was  $\Theta_D \approx 210 \text{ K}$ ; used values  $s = 17$  or  $12,5\mu_B$  for different thickness of intermediate layer) the authors [32] received very interesting results regarding the temperature dependence  $\rho_{ph}(T)$  and  $\rho_m(T, B)$ . It was established that  $\rho(T, 0)/\rho_0$  changes from 1,35 ( $T \cong 0 \text{ K}$ ) to 2,07 ( $T \cong 300 \text{ K}$ ), and  $\rho(T, B)/\rho_0$  – changes from 1,0 ( $T \cong 0 \text{ K}; B = 12 \text{ T}$ ) to 2,07 ( $T \cong 300 \text{ K}; B = 12 \text{ T}$ ).

Something unexpected had proved the value  $\rho_m(T, B)$  compared with  $\rho_0$ . For example, when  $B = 12$   $\rho_m(T, B)/\rho_0 \cong 0$  (at  $T \approx 0 \text{ K}$ ) and increased to 0,11 (at  $s = 12,5\mu_B$ ) or 0,24 (at  $s = 17\mu_B$ ). We emphasize that in this case we are talking about SDSE magnetic moments of granules bcc Fe in the matrix s.s. Ag (Fe). The authors take into account the possible SDSE on magnet moments domain s.s.

As was noted by us earlier in [7] was proposed by-

phenomenological model for longitudinal strain coefficient, which was approbation for example granular film systems based on Fe and Pt. It has been an interesting conclusion as to what the main contribution to the total value  $\gamma^p$  gives only s.s.  $\text{Me}_1(\text{Me}_2)$ , i.e. granular matrix alloy. This can qualitatively explain based on the concept of [40] and the perceptions of ballistic carried charger. According to [40], the strain resistor, which as a leading carried phase metal particles in, for example, the dielectric matrix strain effect is realized in the interval of one mean free path of electrons ( $\lambda_0$ ). Since the size of the granules will always be less  $\lambda_0$  ( $r_0/\lambda_0 < 1$ ) we conclude that in within granules ballistic electron-carrying mechanism, so we can write:

$$\gamma_1^{\lambda_0} = \frac{1}{\lambda_0} \frac{\partial \lambda_0}{\partial \varepsilon_i} = 0$$

At the same location in s.s. normal conductivity mechanism is implemented, which gives the main contribution to the total value of SC.

We have studied the temperature dependence of the electrophysical properties (resistivity and TCR) granular alloy, formed by methods simultaneously ((Ag+Fe)/S) or so-layer (Fe/Ag/Fe/S) condensing of component at the  $T_s = 400 \text{ K}$  followed by annealing at the  $T_a \cong 800 \text{ K}$ . Diffraction and electron microscopic studies indicate that in the condensation process fcc s.s. Ag (Fe) is formed (Fig. 2), although it is known (see, for example, cited our work [23], which illustrate deviation from the rules Vegard in s.s. Ag (Fe), that the solubility of atoms of Fe in the fcc lattice Ag is very limited.

At the same time, an analysis of the relative intensity of lines (111) and (222) (Fig. 2a, c) does not preclude the conclusion that at the us-deposition state to some extent saved individuality of separate layers, and redistribution of lines intensities associated with the coincidence of interplanar distances (100) Ag and (110) Fe, (220) Ag and (200) Fe, (222) Ag and (211) Fe.

The lattice parameters will have value  $a(\text{Ag}) = 0,4080 \text{ nm}$  (in bulk Ag  $a_0 = 0,4086 \text{ nm}$ ) and  $a(\alpha\text{-Fe}) = 0,2871 \text{ nm}$  (in a bulk  $\alpha\text{-Fe}$   $a_0 = 0,2866 \text{ nm}$ ) to coincide with the results of works [23, 34-36], in which phase analysis was carried out on the XRD [33, 36] or electron diffraction [34, 35].

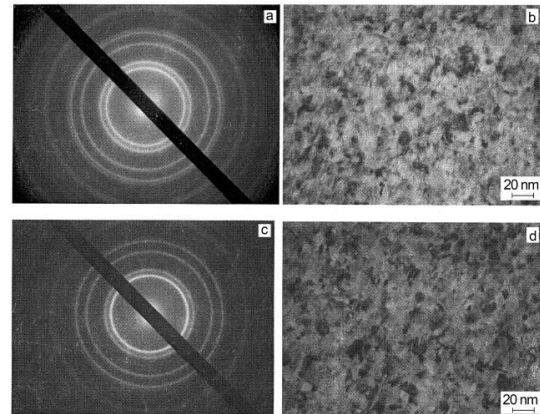


**Fig. 2** – The diffraction of electrons (a, c) and microstructure (b, d) of granular film alloys, which formed at the layered condensation of systems Fe(5)/Ag(10)/Fe(10)/S

At the same time, the mixed ionic of multilayers some relatively small dose ions Xe [34] or Ar [35] also observed a two-phase state fcc Ag + bcc Fe. Note also that in Fig. 2 is not fixing clearly granules  $\alpha$ -Fe, as in works [20, 35] (the results of [20, 21] can not be consider as an example the formation of perfect granular system since authors have implemented Fe clusters in Ag matrix).

In [23, 35] observed granules irregular shape as in Fig. 2. The authors [36] modeled of granules as spherical and ellipse particles, which have a complex structure (Fig. 3) and can touch.

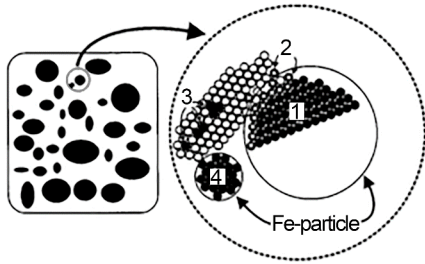


**Fig. 3** – Structure of granules Fe in s.s. Ag(Fe): 1 – bulk  $\alpha$ -Fe; 2 – interface on boundary granule  $\alpha$ -Fe and s.s. (Ag); 3 – Fe atoms in lattice s.s. Ag(Fe); 4 – granule  $\gamma$ -Fe. From the work [36]

Temperature dependence  $\rho$  and TCR for samples formed by layer condensation us three-layer film Fe/Ag/Fe/S, shown on Fig. 4.

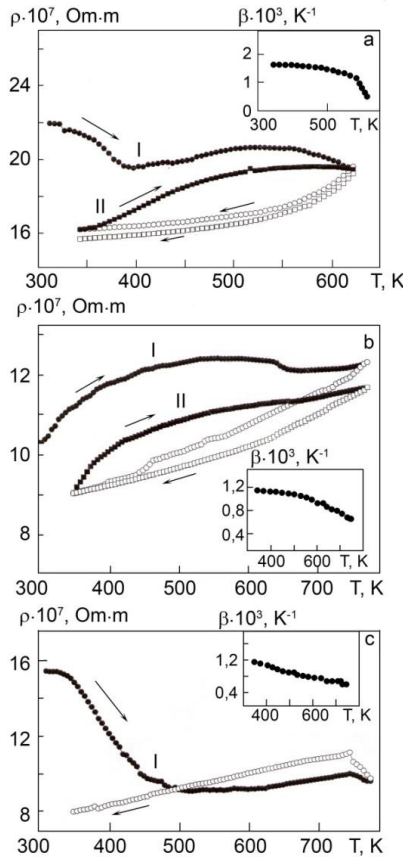


**Fig. 4** – Temperature dependence  $\rho$  i TCR for film systems, which formed us three-layer film: Fe(5)/Ag(5)/Fe(5)/S (a); Fe(5)/Ag(10)/Fe(10)/S (b) and Fe(10)/Ag(30)/Fe(10)/S (c). I, II – numbers of annealing cycles

The significant distinction value  $\rho$  accordance our data and data [14], that is connected with the range of thickness differs by one or two orders of magnitude, the grain boundary and surface scattering of electrons (see, for example, [42]) makes a significant contribution to the resistivity. In work [41] we have been made on the example of film systems based on Fe and Co, Cu and Ag approbation of ratio (2) and received a good correlation of experimental and calculated data. The results [43] indicate on the same correlation in the case of films based on Ag and Fe. Summarized results and some data of work [14] (Table 1).

### 2.3 Magnetoresistance Properties

In this section we summarize of known literature data about observation GMR effect in granular s.s. Ag (Fe) (Table 2). On Fig. 5 depending GMR in granular multilayers  $[\text{Ag}(d_{\text{Ag}})/\text{Fe}(d_{\text{Fe}})]_{40}/\text{SiO}_2(10)/\text{Si}$  versus film thickness of Fe in the initial state at three film thicknesses Ag [25].

Note also that the relatively small value GMR in [26] related to the large thickness of the intermediate layer  $d_{\text{Ag}}$ , because even when the thickness of the intermediate layer  $d_{\text{Ag}} > 1,0$  nm GMR decreases sharply [25] through impossibility of antiferromagnetic interaction between the magnetic layers.

## 3. FILM MATERIALS BASED ON Fe AND Au

### 3.1 Structural and Phase State

Systematic research of phase composition of films based on Fe and Au were carried in works [44-50], the authors have observed the formation of fcc s.s. Au(Fe) with lattice parameters  $a = 0.400-0.404$  nm [44, 45, 49, 50] that with increasing temperature decreases to 820 K [45] to the value of  $a = 0.399$  nm. Obviously, this decrease can be explained by streamlining processes in s.s. Au(Fe) at annealing the samples. Note that the authors [48] observed in s.s. Au(Fe) value of  $a = 0.417$  nm, which, in their view, means the possibility of forming fcc s.s. not only based on Au, but  $\gamma$ -Fe.

According data [44, 46] at increasing the concentration to 80 at. % Fe [44] or to 65 at. % Fe [46] is a phase transition to s.s.  $\alpha$ -Fe(Au) (according to our data [50] this transition occurs at  $c_{\text{Fe}} > 60$  at. % (Fig. 6), confirming the result of [46]). Note that the authors [49] also observed the beginning of a phase transition with increasing  $c_{\text{Fe}}$  36 to 66 at. %. Transition of s.s. Au(Fe)  $\rightarrow$  s.s.  $\alpha$ -Fe(Au) accompanied by dispersing the crystal structure and can be interpreted us quasicrystalline [50]. The authors [44, 46] indicate that s.s. Au(Fe) disordered to a concentration of about 50 at. % Fe, when the nanoclusters are formed on the basis of an orderly s.s. Fe(Au) of the L10 structure [47, 48] and tetragonal lattice parameters  $a = 0.367$  and  $c = 0.360$  nm [47]. In the case [47] L10 phase formed in multilayers  $[\text{Fe}_1\text{ML} / \text{Au}_1\text{ML}]_{100}$ .

Note that the L10 structure is formed based on transition (Fe, Co, Mn) and noble (Pt, Pd, Au, Ir, Rh) metals. As you can see, the list is not noble metals Ag and this means that in s.s.  $\alpha$ -Fe(Ag) do not occur ordered processes, although phase (concentration) transition fcc s.s. Ag(Fe)  $\rightarrow$  bcc s.s.  $\alpha$ -Fe(Ag) occurs at the when  $c_{\text{Fe}} < 50$  at. % (see, section 1.1).



**Table 1** – Electrophysical properties of granular films

№	Film system in the initial state (nm)	Total thickness, nm	$c_{Fe}$ , at. %	$T_m$ , K	$T_a$ , K	$\rho \cdot 10^7$ , Ohm·m	$\beta \cdot 10^3$ , K <sup>-1</sup>
1	Fe(5)/Ag(5)/Fe(5)/S	15		300	300	15,64	1,6
				500	500	16,52	1,4
				800	800	19,41	0,4
2	Fe(5)/Ag(10)/Fe(10)/S	25		300	300	9,03	1,2
				500	500	9,65	1,1
				800	800	11,25	0,7
3	Fe(10)/Ag(30)/Fe(10)/S	30		300	300	7,96	1,2
				500	500	8,84	1,1
				800	800	9,95	0,6
4	Fe/Ag/S [14]	200-1000	20	300	320	3,13	–
					470	1,60	
					620	1,03	
					720	0,82	

$T_m$  – measurement temperature

**Table 2** – Effect of GMR in film systems based on Ag and Fe

№	Thickness of film, nm	$c_{Fe}$ , at. %	$T_m$ , K	$T_a$ , K	GMR, %	Magnetic field induction, T	Literature sources
1	200-1000	4 17 43 71	4,2	320	14,6	to 2,0	[14]
					30,3		
					3,9		
					1,18		
2	200-1000	13 20 20 20	4,2	320	28,6	to 2,0	[14]
			77	570	10,2		
			300	–	4,22		
			300	670	0,70		
3	200	29	–	670 in magnetic field 0,3 T	7,0	to 2	[19]
4	[Ag( $d_{Ag}$ )/Fe( $d_{Fe}$ )] <sub>40</sub> /SiO <sub>2</sub> /Si $d_{Ag} = 1,2$ ; 1,5; 2,3 nm	20 – 33	4,2	–	14,0	6	[24, 25]*
		49 – 65	300	–	0,40	6	
5	Ag(2)/[Fe(2)/Ag(4)/Co(2)/Ag(4)] <sub>3</sub> /Ag(2)/Si(100); 40	51	–	–	0,2	to 0,06	[26]
6	Ag <sub>1-x</sub> Fe <sub>x</sub>	10 – 30	4 – 300	–	to 16	to 5	[28]
7	Granular s.s.(Ag)Fe	24	–	–	7,0	1,5	[29]
		32	–	–	10,0	1,5	
8	Granular s.s.(Ag)Fe	15	10	–	1,025	1,6	[30]
		25	10	–	0,30	1,6	
9	Granular multilayer Fe/Ag	–	4,2	–	26,0	to 12	[32]
		–	120	–	15,5		
		–	290	–	5,55		

\* Due to the low measurement temperatures in the multilayers likely not stabilized granular s.s. The authors particularly emphasize the important role thickness of Fe; when reaching  $d_{Fe} > 1,2$  nm GMR at 4.2 K is less than GMR at 300 K.

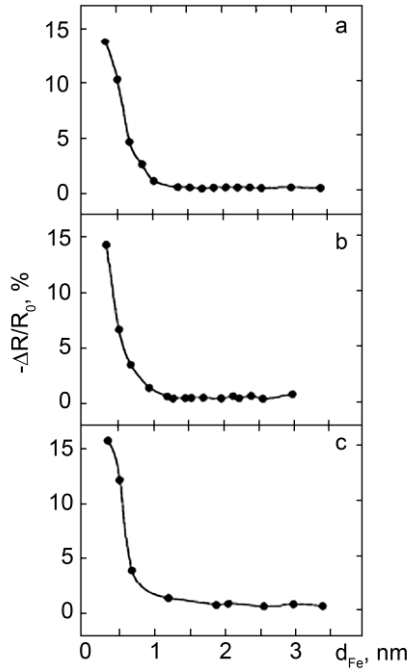


**Fig. 5** – The dependence of GMR versus thickness layer Fe at the temperature measurement 4,2 K with different thickness layer Ag in multilayer [Ag/Fe]<sub>40</sub>/S: 1,2 (a); 1,5 (b) and 2,3 nm (c). From the work [25]

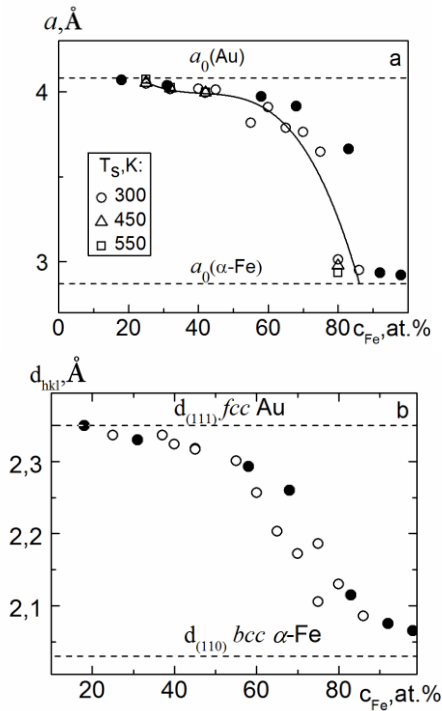


**Fig. 6** – Dependence fcc lattice parameter (a) and space distance for (111) s.s. Au(Fe) and (110) s.s.  $\alpha$ -Fe(Au) at the 300 K. • – data of [44]. From the work [50]

**3.2 Electrophysical Properties**

Electrophysical properties (resistivity, TCR and SC) of granular film systems based on Fe and Au are poorly understood. A possible explanation for this may be the fact that these properties are related film systems

based on Ag and Fe at present sufficiently studied and the results can be extrapolated on the case of granulated film alloy s.s. Au(Fe) or s.s.  $\alpha$ -Fe(Au). While our results in [25] for the concentration of Au(Fe) in the transition region for Au(Fe)  $\rightarrow$  bcc  $\alpha$ -Fe(Au) have shown a possibility of applying the formula (1) and (2) in the example of [25]

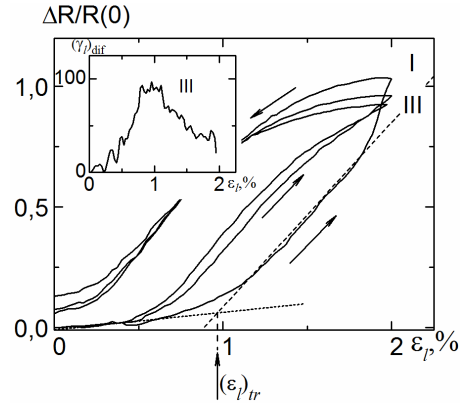


**Fig. 7** – To explain the methodology the determination of  $\epsilon_{tr}$  based on strain dependency. On the insert- dependence  $(\gamma)_{air}$  versus  $\epsilon_l$  for s.s.Au(Fe) at the concentration  $c_{Fe} = 70$  at.%. I – III – the numbers of strain cycles

When studying the strain effect film samples were obtained by simultaneous condensation in vacuum  $10^{-4}$  Pa known weight Fe and Au with a predetermined calculated concentration of the component ( $c_{Fe} = 20-85$  at. % with step 5 at. %). The accuracy of the calculated concentrations controlled by method XRMA, which made it possible to examine the concentration dependence  $\gamma_1$  of fcc s.s. Au(Fe), bcc s.s.  $\alpha$ -Fe(Au) and quasi-amorphous alloy based on  $\alpha$ -Fe. For the realization this phase composition of sample the thickness should be 20-30 nm. At the condensation layer can be implemented phase composition s.s. Au (Fe) +  $\alpha$ -Fe (Au) or s.s.  $\alpha$ -Fe (Au) + fcc Au.

The technique of measurement SC is described in detail by us in works [51] and [52]. The values of strain  $\epsilon_{tr}$ , at which the transition from elastic to plastic strain, we determined the point of intersection of two areas contiguous to strain dependence (example of this procedure is shown on Fig. 7). Experimental studies of the structure and strain effect were performed after cooling of the samples at the 300 K. In addition to clarifying the value  $\epsilon_{tr}$  used data of works [53-55], and to take account of size effects on mechanical properties used analysis, carried out in work [56].

Diffraction and electron microscopic studies indicate that the film samples thickness of 20-40 nm immediately after simultaneous condensation component stabilizes the fcc phase s.s. Au(Fe) to a concentration  $c_{Fe} \approx 55$  at. % depending on the thickness of the sample, while at the values  $c_{Fe} \approx 65-85$  at. % – quasi-amorphous and crystalline s.s.  $\alpha$ -Fe(Au). The dependence of the lattice parameter of these s.s versus  $c_{Fe}$ , of which is consistent with the data [44] and [45], shown in Fig. 6a. More clearly fcc lattice transformation is illustrates dependence interplanar distances or effective interplanar distance which calculated by the first diffraction peak (Fig. 6b). At the same time we have not observed s.s.  $\gamma$ -Fe(Au), as is the case [48].

Series micropictures and diffraction patterns (Figures 8, 9) illustrate the change in structural phase state of films by changing the concentration of components. Attention is drawn status of ultra-dispersion state samples at  $c_{Fe} \cong 55-75$  at. %, which is accentuated attention in the analysis of the results studying strain effect. On the Fig.10 are examples of strain dependency  $\Delta R/R(0)$  and  $(\gamma)_{dif}$  versus  $\epsilon_l$ , where  $\Delta R = R(\epsilon_l) - R(0)$ ;  $R(\epsilon_l)$  and  $R(0)$  – electric resistance at the strain  $\epsilon_l$  and  $\epsilon_l = 0$ .

As already noted, depending on the maximum  $(\gamma)_{dif}$  versus  $\epsilon_l$  also observed by us earlier [52, 60] the example of other film materials. The nature of it is related to the transition from elastic to plastic strain of the samples.

Results of processing the strain dependency on Fig. 11 are presented.

Of them follows that in the concentration range  $c_{Fe} \cong 55-75$  at. % there is an abnormal increase in value  $(\gamma)_{int}$ . This result can be explained by dispersing s.s.-(Au) at the increasing values  $c_{Fe}$  (Fig. 8). According to theoretical models of effective free path of electrons by C. Tellier and A. Tosser [3] value  $(\gamma)_{int}$  completely determined by the grain boundary scattering of electrons, because their surface scattering affects only the character of the dependence  $(\gamma)_{int}$  from the thickness of the film sample. Thus, increasing the efficiency of grain boundary scattering of electrons in the concentration range  $c_{Fe} \cong 55-75$  at. % is a cause of abnormal increase in value  $(\gamma)_{int}$ .

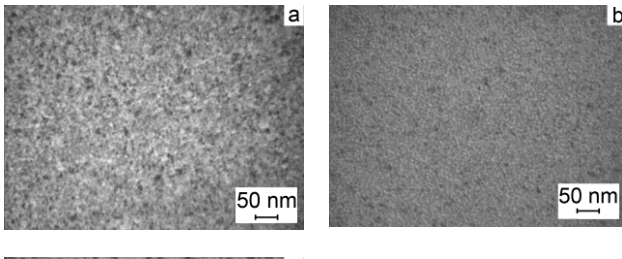


**Fig. 8** – Microstructure of films fcc s.s. Au(Fe) and s.s.  $\alpha$ -Fe(Au). Concentration, at.% Fe: a – 42; b – 65 and c – 80. From the work [50]

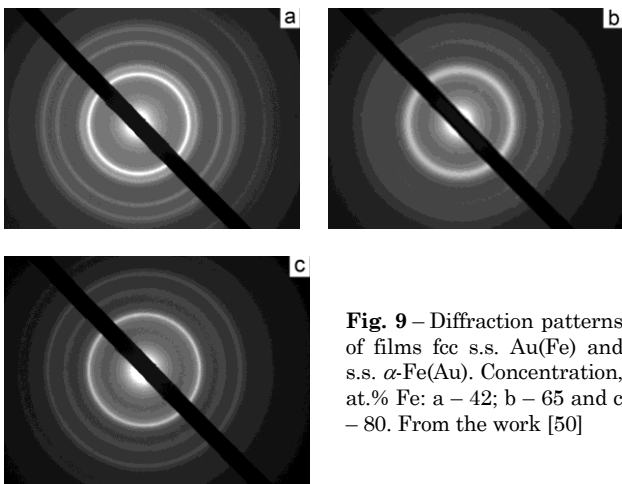


**Fig. 9** – Diffraction patterns of films fcc s.s. Au(Fe) and s.s.  $\alpha$ -Fe(Au). Concentration, at.% Fe: a – 42; b – 65 and c – 80. From the work [50]

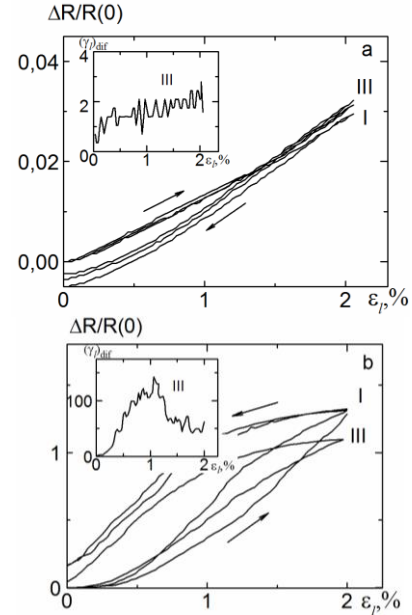


**Fig. 10** – The examples of strain dependencies for the films fcc s.s. - (Au). Concentration, at. % Fe: a – 32; b – 55. On the insert- dependence  $(\gamma)_{dif}$  versus  $\epsilon_l$ . From the work [50]

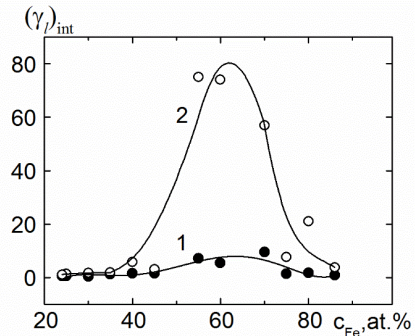


**Fig. 11** – Dependence  $(\gamma)_{int}$  versus  $c_{Fe}$  at the elastic (1) and plastic (2) strain of samples based on Fe and Au. From the work [50]

Based on the basic ratio for the strain longitudinal coefficient

$$(\gamma_l)_{int} = -\frac{1}{\lambda_0} \frac{\Delta\lambda_0}{\Delta\epsilon_l} + 2(1 + \mu_f),$$

we can conclude the main contribution to the value  $(\gamma)_{int}$  strain coefficient of  $\lambda_0 \left( -\frac{1}{\lambda_0} \frac{\Delta\lambda_0}{\Delta\epsilon_l} \right)$ , because the second term in (1) so-called the geometric factor makes contributions up to 3 units. The decrease  $\Delta\lambda_0$  is due to direct dependence on  $\lambda_0$  versus  $\epsilon_l$  and indirect dependence  $\lambda_0$  versus  $\epsilon_l$  on the parameters  $p$  and  $r$ :  $(\Delta\lambda)_p$  and  $(\Delta\lambda)_r$ .

In works [58, 59] analyzed the question of fundamental nature, namely the influence on the conductivity interface SDSE three-layer epitaxial structures Fe/Au/Fe/GaAs(001). In the works are several important parameters (coefficients of reflectivity, interfaces, the lifetime of the spin orientation; diffusivity parameters; the mean free path of electrons of opposite spin orientation, etc.) were present.

Notice that the authors [60] also analyzed the role of



interface scattering multilayers Au/Fe/Au/Fe. Experimental results for  $\rho$  (Fig. 12) and GMR are in good agreement with the theoretical model proposed by the authors for  $\rho$  and GMR.

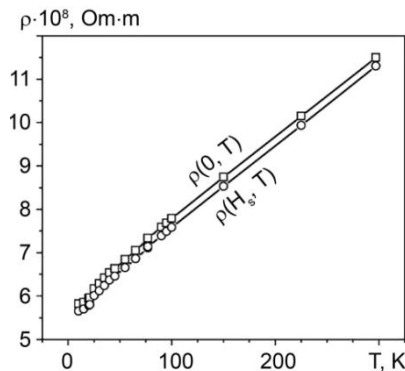


**Fig. 12** – Experimental field- and temperature-dependent resistivities. From the work [60]

### 3.3 Magnetoresistive Properties

Magnetoresistive as electrical, properties remain poorly understood, although a wide range of magnetic properties studied sufficiently (see, for example, [5, 48]). The uniqueness of results of these studies is that the authors measure the shape and magnetic properties of samples in which magnetic granules with different phase composition:  $L1_2$  ( $\text{Fe}_3\text{Au}$ ),  $L1_0$  ( $\text{FeAu}$ ) and  $L1_1$  ( $\text{FeAu}_3$ ). It was established that the saturation magnetization phase  $L1_2$  almost 15 times (at 300 K) higher compared to the phase  $L1_1$ .

The authors [49] carried investigation MR of nanodimension film systems based on Fe and Au, obtained layered condensation (total thickness of samples to 50 nm), followed by annealing at  $T_a = 700\text{-}900$  K during 30 min.

Analysis of diffraction patterns (Fig. 13) indicates that even at low thickness Fe layers ( $2d_{\text{Fe}} \cong 10$  nm) in the initial system Fe/Au/Fe/S, Fe atoms are not completely solution in the layer Au. This is confirmed by the

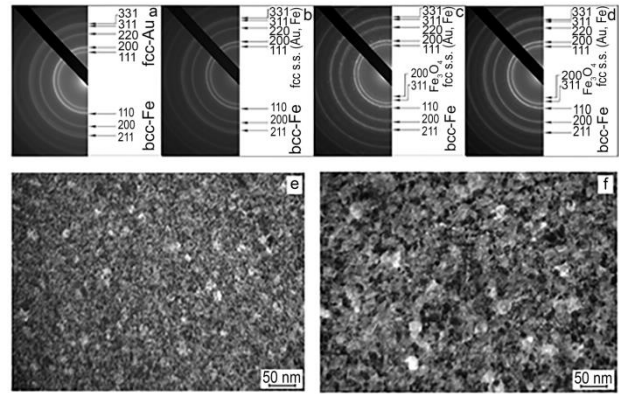


**Fig. 13** – Diffraction pattern (a-d) and crystalline structure (e, f) of thin film system Fe(5)/Au(25)/Fe(5)/S as deposition (a, e) and annealing to 700 (b), 800 (c) and 900 K (d, f). From the work [49]

fact that there is a redistribution of the intensities of lines (111) and (200) s.s. Au (Fe), since  $I_{200} > I_{111}$ , because of the coincidence lines (110)  $\alpha$ -Fe and (200) s.s. Au(Fe). Obviously, with such a phase composition should not expect formation of perfect granulated alloy and, hence, relatively large values MR or GMR.

Confirmation of this conclusion can serve as research results of GMR in multilayers Au/Fe/Au/Fe [61], which are presented in Fig. 15.

### 4. CONCLUSIONS

Analysis of published data and own results allows us conclusions.

1. Currently there is a need streamlining terminology and conceptual apparatus and therefore, the following designations:

- $(\text{Me}_1 + \text{Me}_2)/\text{S}$  – simultaneous condensation of two metals;
- $\text{Me}_1/\text{Me}_2/\text{S}$ ,  $[\text{Me}_1/\text{Me}_2]_n/\text{S}$  – double-layer film or multilayer, formed layered condensation method;
- $(\text{Me}_1 \text{ or } \text{D})/\text{IF } \text{Me}_2/(\text{Me}_1 \text{ or } \text{D})/\text{S}$  – nanocomposite material with separate layer of magnetic island;

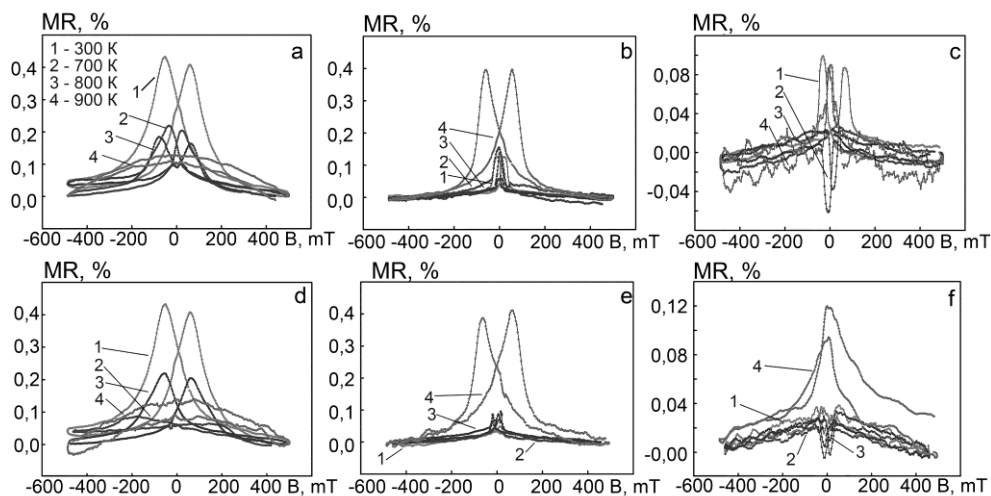


**Fig. 14** – Magnetoresistance dependence vs. applied field for film systems Fe(5)/Au(25)/Fe(5)/S (a-c) and Fe(10)/Au(15)/Fe(10)/S after condensation and heat treated to 700, 800, 900 K. Magnetic field lying in longitudinal (a, d), transverse (b, e) and perpendicular geometries (c, f). From the work [49]

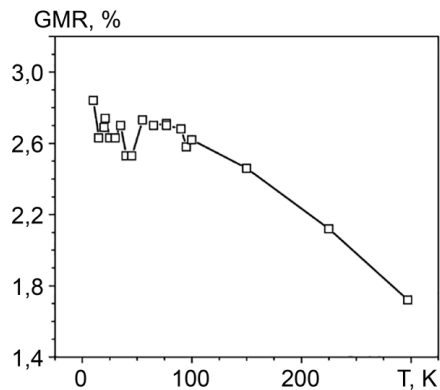


Fig. 15 – Temperature dependence of GMR in multilayers Au/Fe/Au/Fe. From work [61]

- $\text{Me}_1(\text{Me}_2)$  – disordered s.s. atoms  $\text{Me}_2$  in  $\text{Me}_1$ ;
- s.s.  $(\text{Me}_1, \text{Me}_2)$  – ordered s.s. atoms  $\text{Me}_2$  in  $\text{Me}_1$ ;
- $\text{Me}_1(\text{Me}_2) + \text{G}$ ;  $(\text{Me}_1, \text{Me}_2) + \text{G}$  – granular s.s.;
- $(\text{Me}_1)_x(\text{Me}_2)_y$  – intermetallide.

2. We should not designate grained film alloys symbols  $(\text{Me}_1-\text{Me}_2)$ ,  $\text{Me}_1/\text{Me}_2$  та  $(\text{Me}_1)_x(\text{Me}_2)_{1-x}$ , because they do not meet the physical nature of alloys.

## REFERENCES

1. A.E. Berkowitz, J.R. Mitchell, M.J. Carey, A.P. Young, S. Zhang, F.E. Spada, F.T. Parker, A. Hutten, G. Thomas, *Phys. Rev. Lett.* **68**, 3745 (1992)
2. A.Fert, J. Duvail, T. Valet, *Phys. Rev. B* **52**, 6513 (1995)
3. K.Yu. Guslienko, *Phys. Solid State* **40**, 10, 1697 (1998)
4. A.B. Granovskii, A.V. Vedyayev, A.V. Kalitsov, *Fizika Tverdogo Tela* **37**, 337 (1995)
5. P. Mukherjee, P. Manchanda, P.Kumar, L. Zhou, M.J. Kramer, A. Kashyap, R. Skomski, D. Sellmyer, J.E. Shield, *ACS Nano* **8**, 8, 8113 (2014); A. B. Granovsky, M. Il'in, A. Zhukov, V.Zhukova, Kh. Gonzales, *Phys. Solid State* **53** No 2, 320 (2011)
6. S.I. Protsenko, L.V. Odnodvoret, I.V. Cheshko, *Visnyk SumDU. Seria: Fizyka, matematyka, mekhanika* **1**, 22 (2008)
7. L.V. Odnodvoret, M.O. Shumakova, I.Yu. Protsenko, Yu.M. Shabelnyk, N.I. Shumakova, *Proceedings of the international conference nanomaterials: applications and properties* **3**, 1, 01NTF09 (2014)
8. C. Rizal, Y. Ueda, B.R. Karki, *J. Nano-Electron. Phys.* **4**, 01001 (2012).
9. L.V. Odnodvoret, *Proceedings of the international conference nanomaterials: applications and properties* **3**, 1, 01NTF08 (2014).
10. D.M. Kondrahova, Yu.M. Shabelnyk, O.V. Synashenko, I.Yu. Protsenko, *Usp. Fiz. Met.* **13**, 241 (2012)
11. P. Grunberg, J. Barnas, F. Saurenbach, J.A. Fub, A. Wolf, M. Vohl, *J. Mag. Magn. Mater.* **93**, 58 (1991)
12. C. Rizal, B.B. Niraula, *J. Nano-Electron. Phys.* **7** No 4, 04068 (2015).
13. X.Peng, A.Morrone, K.Nikolaev, M. Kief, M. Ostrowski, *J. Mag. Magn. Mater.* **321**, 2902 (2009)
14. J.-Q. Wang, G. Xiao, *Phys. Rev. B* **49**, 3982 (1994)
15. I. Bakonyi, L. Peter, *Prog. Mater., Sci.* **55**, 107 (2010)
16. S.A. Nepijko, D. Kutnyakhov, S.I. Protsenko, L.V. Odnodvoret, G.Schönhense, *J. Nanopart. Res.*, **13**, 6263 (2011)
17. D.L. Peng, J. Wang, L. Wang, X. Liu, Z. Wang, Y. Chen, *Sci. China Phys. Mech. Astron.* **56**, 15 (2013)
18. Y. Ju, C. Xu, Z.Y. Li, *J. Magn. Magn. Mater.*, **223**, 267 (2001)
19. J.G. Na, C.T. Yu, X.G. Zhao, W.Y. Lai, H.L. Luo, J.G. Zhao, *J. Appl. Phys.*, **76**, 6484 (1994)
20. K. Sumiyama, T. Hihara, S.A. Makhlof, K. Wakoh, M. Sakurai, Y. Xu, T.J. Konno, S. Yamamuro, K. Suzuki, *Mater. Sci. Eng. A* **217-218**, 340 (1996)
21. G.-F. Hohl, T. Hihara, M. Sakurai, T. J. Konno, K. Sumiyama, F. Hensel, K. Suzuki, *Appl. Phys. Lett.* **66**, 385 (1995)
22. S. Kahl, H.-U. Krebs, *Phys. Rev. B* **63**, 172103-1 (2001)
23. R.L. Zong, S.P. Wen, F. Zeng, Y. Gao, C. Song, B. He, F. Pan, *Appl. Surf. Sci.* **253**, 2993 (2007)
24. L. Shuxiang, Yu. Chengtao, Y. Minglang, L. Wuyan, W. Yizhong, *Chin. Phys. Lett.* **11**, 775 (1994)
25. S. Li, C. Yu, W. Lai, Y. Wang Y., Yan M. *J. Appl. Phys.* **78**, 405 (1995)
26. C. Birlikseven, A. Bek, H.Z. Durusoy, *Turk. J. Phys.* **23**, 1101 (1999)
27. D. Bisero, E. Angeli, F. Spizzo, P. Vavassori, F. Ronconi, *J. Magn. Magn. Mater.* **262**, 116 (2003)
28. P. Allia, M. Coisson, F. Spizzo, P. Tiberto, F. Vinai, *Phys. Rev. B* **73**, 054409 (2006)
29. M. Tamisari, F. Spizzo, M. Sacerdoti, G. Battaglin, F. Ronconi, *J. Nanopart. Res.* **13**, 5203 (2011)
30. V. Iannotti, S. Amoroso, G. Ausanio, A.C. Barone, C. Campana, C. Hison, L. Lanotte, *J. Mater. Process. Technol.* **208**, 409 (2008)
31. J. Alonso, M.L. Fdez-Gubieda, G. Sarmiento, J.M. Barandiaran, A. Svalov, I. Orue, J. Chaboy, L. Fernandez Barquin, C. Meneghini, T. Neisius, N. Kawamura, *Appl. Phys. Lett.* **95**, 082103 (2009)
32. M. Csontos, J. Balogh, D. Kaptas, L.F. Kiss, A. Kovacs, G. Mihaly, *Phys. Rev. B* **73**, 184412 (2006)
33. Z. Xiao-Ying, L. Xue-Jing, Z. Fei, P. Feng, *Trans. Nonferrous Met. Soc. China* **20**, 110 (2010)
34. X.Y. Li, L.T. Kong, B.X. Liu, *Phys. Rev. B* **72**, 054118 (2005)
35. A.K. Srivastava, S. Amirthapandian, B.K. Panigrahi, A.

- Gupta, R.V. Nandedkar, *Nucl. Instrum. Methods Phys. Res., Sect. B* **244**, 359 (2006)
36. C. Aloy, B. Stahl, M. Ghafari, H. Hahn, *J. Appl. Phys.* **88**, 4212 (2000)
37. J. M. Soares, J. H. de Ararjo, F.A.O. Cabral, J.A.P. da Costa, J.M. Sasaki, *Mat. Res.* **7**, 513 (2004)
38. M.K. Roy, P.M.G. Nambissan, H.C. Verma, *J. Alloys Compd.* **345**, 183 (2002)
39. D. A.Hite, S. E. Russek, D.P. Pappas, *J. Appl. Phys.* **94**, 621 (2003)
40. E.M. Winkler, G.K. Steenvoorden, *Thin Solid Films* **152**, 487 (1987)
41. D.M. Kondrakhova, O.V. Vlasenko, L.V. Odnodvoretz, O.V. Pylypenko, I.Yu.Protsenko, O.P. Tkach, Yu.M. Shabelnyk, *Book of abstracts of 5th International Scientific Conference "FMMN-2011". – Kharkov. – 12 - 14 October, 6 (2011)*
42. Protsenko S.I., Odnodvoretz L.V., Protsenko I.Yu.: *Future strain properties of multilayer film materials. In book: Nanocomposites, Nanophotonics, Nanobiotechnology, and Applications*, **156**, 345 (Springer: Switzerland: 2015)
43. Yu.M. Shabelnyk: *Physical properties of thin granular alloys based on magnetic and noble metals*. Dissertation, Sumy State University (2015)
44. Y. H. Hyun, Y.P. Lee, Y.V. Kudryavtsev, R. Gontarz, *J. Korean Phys. Soc.* **43**, 625 (2003)
45. E. Bosco, P. Rizzi, M. Baricco, *Mater. Sci. Eng. A* **375–377**, 468 (2004)
46. P. Mukherjee, L. Zhou, M.J. Kramer, J. E. Shield, *Appl. Phys. Lett.* **102**, 243103 (2013)
47. K. Takanashi, S. Mitani, M. Sano, H. Fujimori, H. Nakajima, A. Osawa, *Appl. Phys. Lett.* **67**, 1016 (1995)
48. P. Mukherjee, Y. Zhang, M. J. Kramer, L. H. Lewis, J. E. Shield, *Appl. Phys. Lett.* **100**, 211911 (2012)
49. I.V. Cheshko, I.M. Pazukha, S.I. Protsenko, Yu.M. Shabelnyk, D.V. Shapko, *Proceedings of the International Conference «Nanomaterials: applications and properties», the Crimea, Ukraine, 16-21 September 2013*, **2**, 1, 01001-1 (2013)
50. O.V.Pylypenko, L.V.Odnodvoretz, M.O.Shumakova, I.Yu.Protsenko, *Problems Atomic Sci. Technol.* **5** (2016).
51. L.V. Odnodvoretz, S. I. Protsenko, O.V. Synashenko, D.V. Velykodnyi, I.Yu. Protsenko, *Cryst. Res. Technol.* **44**, 1, 74 (2009)
52. S.I. Protsenko, D.V. Velykodnyi V.A. Kheraj, M.S. Desai, C.J. Panchal, I.Yu. Protsenko, *J. Mater. Sci.* **44** No 18, 4905 (2009).
53. C.A. Neugebauer, *J. Appl. Phys.* **31** No 6, 1096 (1960)
54. I.P. Buryk, D.V. Velykodnyi, L.V. Odnodvoretz, I.E. Protsenko, E.P. Tkach, *Tech. Phys.* **56** No 2, 232 (2011)
55. O.P. Tkach, L.V. Odnodvoretz, S.I. Protsenko, D.V. Velykodnyi, K.V. Tyschenko, I.Yu. Protsenko, *J. Nano-Electron. Phys.* **2**, 1: 22 (2011)
56. Y. Choi, S. Suresh, *Acta Materialia*, **50**, 1881 (2002)
57. C.R. Tellier, A.J.Tosser, *Size effects in thin films* (Elsevier: Amsterdam – Oxford – New York: 1982)
58. A. Enders, T.L. Monchesky, K. Myrtle, R. Urban, B. Heinrich, J. Kirschner, X.-G. Zhang, W.H. Butler, *J. Appl. Phys.* **89**, 7110 (2001)
59. T. L. Monchesky, A. Enders, R. Urban, K. Myrtle, B. Heinrich, X.-G. Zhang, W. H. Butler, J. Kirschner, *Phys. Rev. B* **71**, 214440 (2005)
60. K.V.Tyschenko, I.Yu.Protsenko, *Metallofiz. Noveish. Technol.* **34**, 7, 907 (2012)
61. P. Weinberger, J. Zabloudil, R.H. Hammerling, *Phys. Rev. B* **67**, 054404 (2003).